# Modeling the Surface Energy Balance and Soil Moisture at the Atmospheric Radiation Measurement Cloud and Radiation Testbed in the U.S. Southern Great Plains

*J.C. Liljegren, J.C. Doran, J.M. Hubbe, W.J. Shaw, S. Zhong*
*Pacific Northwest National Laboratory*
*Richland, Washington 99352*

*G.J. Collatz*
*National Aeronautics and Space Administration/Goddard Space Flight Center*
*Greenbelt, Maryland*

*D.R. Cook, R.L. Hart*
*Argonne National Laboratory*
*Argonne, Illinois*

## Introduction

We have applied the Simple Biosphere (SiB) model of Sellers et al. (1986) to calculate fluxes of net radiation, sensible, latent, and soil heat for July-August 1994 at a spatial resolution of 6.25 km over the $10^5$ $km^2$ domain of the Cloud and Radiation Testbed (CART) in Kansas and Oklahoma.

We determine the vegetation type for the CART from a database generated by the U. S. Geological Survey (USGS 1990). Soil types were provided by the Atmospheric Radiation Measurement (ARM) Program from the State Soil Geographic (STATSGO) database and mapped into the USDA classifications described by Clapp and Hornberger (1978). To provide the input parameters of temperature, pressure, humidity, wind speed, insolation, and precipitation needed to drive SiB, we use a multiquadric interpolation scheme (Nuss and Titley 1994) to grid measurements from the CART extended observing network, the Oklahoma mesonet, National Weather Service surface stations, and the Arkansas Basin River Forecast Center's NEXRAD Stage III precipitation product. SiB also requires a time-varying Leaf Area Index (LAI) to estimate the biophysical rates that control local evapo-transpiration. We derived estimates of the LAI using a method described by Sellers et al. (1994) which uses the Normalized Difference Vegetation Index (NDVI). We determined NDVI from AVHRR (advanced very high resolution radiometer) imagery provided by ARM.

Although the results of our calculations appeared reasonable, i.e., regions with recent precipitation and large values of NDVI showed greater latent heat fluxes than dry regions with low NDVI values, comparisons with flux measurements from the CART Energy Balance Bowen Ratio (EBBR) stations exhibited considerable deviations from the calculations. The largest differences between modeled and measured fluxes arose from differences in land use: all of the EBBR stations are located in pastures, whereas wheat fields are the dominant land use type in some of the 6.25- x 6.25-km cells containing the EBBR stations. For these locations, the spatially averaged NDVI was quite low since the wheat had been harvested 4-6 weeks earlier but the pastures were generally quite verdant. Consequently, the NDVI input to SiB was not representative of the measurement area, and the modeled fluxes accordingly differed from the measurements.

However, in some areas where pasture was the dominant land use type, the differences between the model and measurements were still larger than we had expected. Because SiB is designed primarily for use at much larger scales (e.g., 3° x 3°) we felt that some adjustment of the vegetation parameters was necessary for comparison with small-scale measurements. We decided to do a simulation at a single location, the CART Central Facility near Lamont, Oklahoma, for an entire growing season (from 1 February to 17 July 1995) in order to determine what adjustments were needed. (We would have continued the simulation for the entire year except that critical instrumentation was destroyed by a lightning strike on 17 July.)

To drive SiB we obtained 30-minute averages of temperature, pressure, relative humidity, wind speed, precipitation, incident solar and thermal-IR fluxes from local CART instrumentation (station E13). To evaluate the model calculations, we obtained 30-minute averages of net radiation, sensible, latent and soil heat fluxes from the local EBBR station. Because these instruments are located in a relatively small pasture completely surrounded by larger wheat fields, we could not use NDVI derived from satellites. To overcome this problem, we used the 665- and 860-nm channels of the down-looking Multi-Filter Radiometers (MFR) mounted on towers over the wheat field and pasture to estimate the local NDVI (Figure 1).

Although the satellite-derived NDVI agreed qualitatively with the local estimate for the wheat field, the satellite values were smaller because of increased reflection in the visible channel from atmospheric aerosols and increased absorption in the near-IR from atmospheric water vapor. To adjust for this, we scaled our local NDVI estimates using the observed minimum and maximum values following Sellers et al. (1994). As shown in Figure 2, the green LAI is initially zero, and only a small value from stems contributes to the total. As the NDVI increases, all leaves are assumed to be green until a maximum is reached in early June. At this point, we assume that the total leaf area remains constant and that the green leaf fraction decreases as the NDVI decreases. We found it

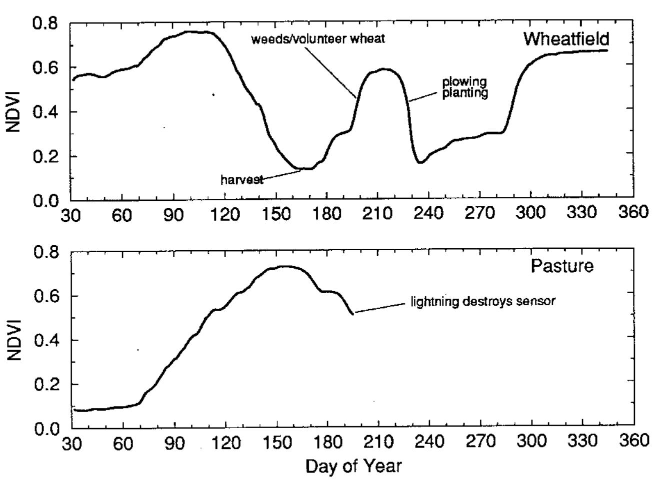


**Figure 1**. Normalized Difference Vegetation Index (NDVI) computed from 665 and 860 nm channels of down-looking multi-filter radiometers for the wheat field and pasture at the CART central facility for 1995.

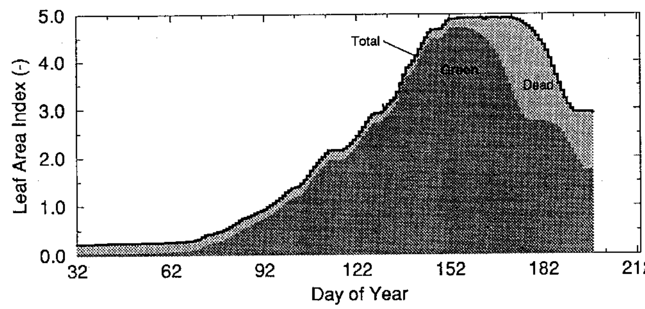


**Figure 2**. Leaf Area Index (LAI) computed from NDVI for the pasture at the CART central facility.

necessary to begin decreasing the total LAI on 19 June to account for cattle grazing in the pasture.

We used a single vegetation type to represent the pasture: $C_3$ grasses. Although the dominant vegetation type probably changes from $C_3$ to $C_4$ type grasses as the average temperature increases (Sellers et al. 1992), we have no information on the relative fractions of these. To achieve agreement with the measurements, we increased the maximum catalytic capacity of the vegetation at 298 K by 25% from 100 to 125 µmol $m^{-2}$ $s^{-1}$. We also found that the low- and high-temperature inhibition functions were unnecessary: the temperature dependence of the assimilation rates was sufficient. Finally, we increased the coefficients of the functions describing the leaf boundary layer resistance $r_b$ and the soil boundary layer resistance $r_d$ over those used in general circulation model (GCM) simulations by factors of 7 and 3, respectively.

In Figure 3, we present scatter plots of the modeled and measured fluxes. The agreement is generally quite good although there are some exceptions. Snow changes the surface albedo but is not always detected by the rain gauge. Consequently, if SiB is unaware of the snow, it over-predicts the net radiation and the sensible heat flux. In addition, if SiB is unaware of the snow, it cannot add the subsequent snow melt to its soil moisture stores. This is evident in Figure 4 in which the soil moisture in the 5-cm thick SiB surface layer is compared with the range of soil moisture measurements from the five EBBR probes at a nominal depth of 5 cm. Snow in February and March was not detected by the rain gauge and consequently SiB could not account for the snow melt: the model soil moisture declines, while the measurements, which are affected by the snow melt, do not. For most of the simulation the modeled soil moisture agrees in both trend and magnitude with the measurements.

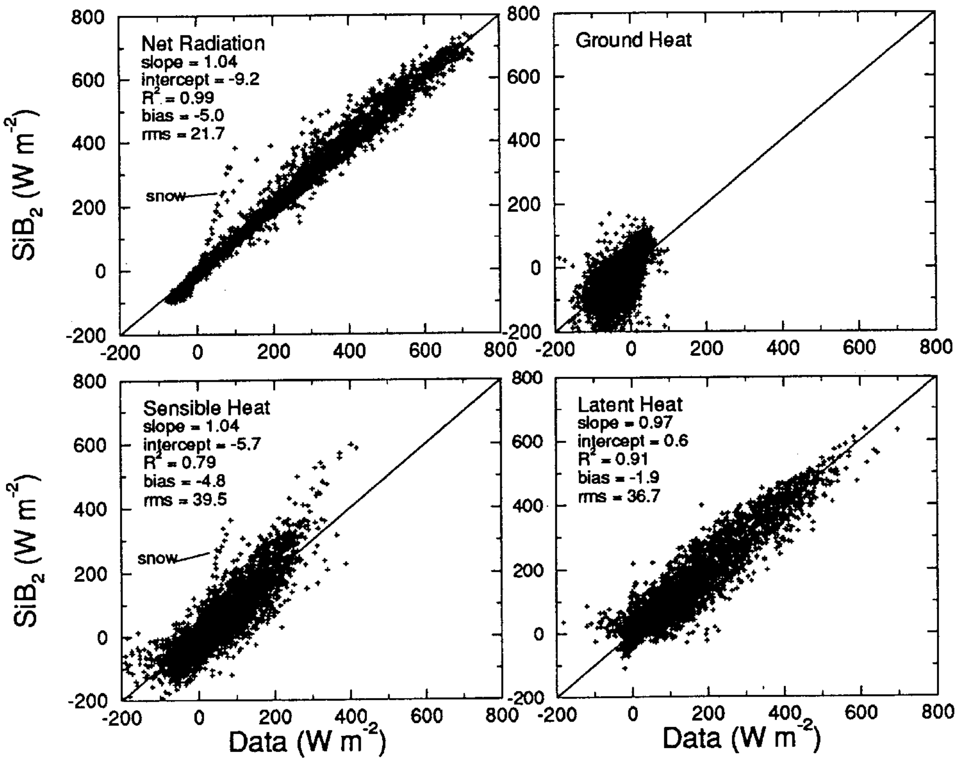


**Figure 3**. Scatter plots of measured and modeled fluxes for 1 February - 17 July 1995.

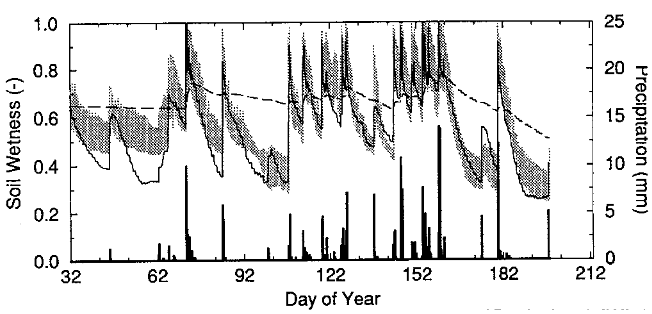


**Figure 4**. Soil wetness from EBBR sensors (grey shading) at 5 cm depth and from SiB surface layer (solid line) and root layer (dashed line). Precipitation amount is indicated by impulses along bottom.

Knowledge of the soil type and thus the hydraulic parameters is critical for modeling the soil moisture. According to the STATSGO database, the Central Facility is an "island" of silty clay loam surrounded by a region of silt loam. To test whether we were using the correct soil type, we ran the simulation using the silt loam parameters and found that the soil surface layer did not exhibit the same drying trend as the data, but instead tracked the root layer moisture. The evaporation from the soil surface was also too large. We attribute this to the fact that the saturated hydraulic conductivity of silt loam is over four times larger than silty clay loam; consequently, the upward diffusion of moisture from the root layer to the surface layer is greatly enhanced for the silt loam soil type. Because the surface soil resistance to evaporation is inversely proportional to soil wetness, the wetter silt loam soil provided a reduced resistance to evaporation.

A measure of the accuracy of SiB for modeling the hydrologic cycle is presented in Figure 5. The cumulative difference (SiB - measurements) in evapo-transpiration is compared with the cumulative measured evapo-transpiration (ET) and the cumulative precipitation. The difference between the cumulative precipitation and ET represents moisture that is either stored in the soil - note that the soil moisture in Figure 4 increases sharply after precipitation events and then declines - or runs off into local streams. In the future, we will try to acquire stream gauge data to check this balance. In any case, the cumulative ET error is a small fraction of the cumulative ET and the precipitation.

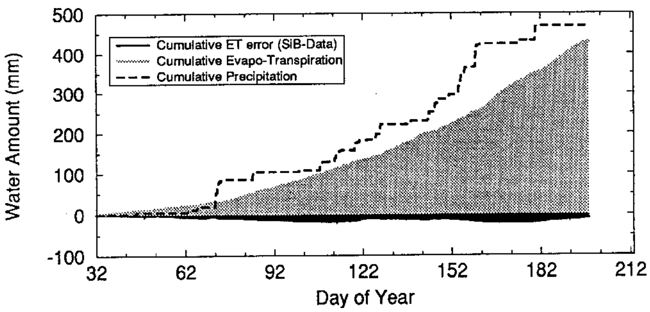


**Figure 5**. Cumulative evapo-transpiration error (dark shading) compared with cumulative evapo-transpiration (light shading) and cumulative precipitation (dashed line).

# References

Clapp, R.B and G.M. Hornberger, 1978: Empirical equations for some soil hydraulic properties. *Water Resour. Res.* **14.4**, 60144.

Nuss, W.A. and D.W. Titley, 1994: Use of multi-quadric interpolation for meteorological objective analysis. *Mon. Wea. Rev.* **121**, 1611-1631.

Sellers, P.J., Y. Mintz, Y.C. Sud and A. Dalcher, 1986: A Simple Biosphere Model (SiB) for use within General Circulation Models. *J. Atmos. Sci.* **43**, 305-331.

Sellers, P.J., M.D. Heiser and F.G. Hall, 1992: Relations between surface conductance and spectral vegetation indices at intermediate (100 $m^2$ to 15 $km^2$) length scales. *J.G.R. FIFE* special issue, **97**:19,033-19,059.

Sellers, P.J., C.J. Tucker, G.J. Collatz, S.O. Los, C.O. Justice, D.A. Dazlich, and D.A. Randall, 1994: A global 1° by 1° NDVI data set for climate studies. Part 2: The generation of global fields of terrestrial biophysical parameters from the NDVI. *Int. J. Remote Sens.* **15**, 3519-3545.

U.S. Geological Survey, 1990: Prototype 1990 conterminous U.S. land cover characteristics data set CD-ROM. EROS Data Center, Sioux Falls, South Dakota.